SLAC-PUB-16246

Multi-gigaelectronvolt, low-energy spread acceleration of positrons in a self-loaded plasma wakefield

S. Corde[1*], E. Adli[1, 2], J. M. Allen[1], W. An[3], C. I. Clarke[1], C. E. Clayton[3], J. P. Delahaye[1], J. Frederico[1], S. Gessner[1], S. Z. Green[1], M. J. Hogan[1], C. Joshi[3], N. Lipkowitz[1], M. Litos[1], W. Lu[5], K. A. Marsh[3], W. B. Mori[4], M. Schmeltz[1], N. Vafaei-Najafabadi[3], D. Walz[1], V. Yakimenko[1], and G. Yocky[1]

[1]SLAC National Accelerator Laboratory, Menlo Park, CA 94025, USA

[2]Department of Physics, University of Oslo, 0316 Oslo, Norway

[3]Department of Electrical Engineering, University of California Los Angeles, Los Angeles, CA 90095, USA

[4]Department of Physics and Astronomy, University of California Los Angeles, Los Angeles, CA 90095, USA

[5]Department of Engineering Physics, Tsinghua University, Beijing 100084, China

*Currently at Laboratoire d'Optique Appliquée, ENSTA Paristech - CNRS UMR7639 - Ecole Polytechnique, 91761 Palaiseau, France

New accelerator concepts must be developed to make future particle colliders more compact and affordable. The Plasma Wakefield Accelerator (PWFA) is one such concept, where the electric field of a plasma wake excited by a charged-particle bunch is used to accelerate a trailing bunch of particles. To apply plasma acceleration to particle colliders, it is imperative that both the electrons and their antimatter counterpart, the positrons, are efficiently accelerated at high fields using plasmas[1]. While substantial progress has recently been reported on high-field, high-efficiency acceleration of electrons in a PWFA powered by an electron bunch[2], such an electron-driven wake is unsuitable for the acceleration and focusing of a positron bunch. Here we demonstrate a new regime of PWFA where particles in the front of a single positron bunch transfer their energy to a substantial number of those in the rear of the same bunch by exciting a wakefield in the plasma. In the process, the accelerating field is altered – self-loaded – so that about a billion positrons gain five gigaelectronvolts (GeV) of energy with a narrow energy spread in a distance of just 1.3 meters. They extract about 30% of the wake's energy and form a spectrally distinct bunch with as low as a 1.8% r.m.s. energy spread. This demonstrated ability of positron-driven plasma wakes to efficiently accelerate a significant number of positrons with a small energy spread may overcome the long-standing challenge of positron acceleration in plasma-based accelerators.

Future high-energy particle colliders operating at the energy frontier of particle physics will be in the range of several trillion electronvolts[3]. The currently proposed machines based on the existing radio-frequency technology, such as the International Linear Collider[4] (ILC) and the Compact Linear Collider[5] (CLIC), are very expensive and tens of kilometers long. Looking beyond these machines, novel methods for building compact and efficient particle colliders, such

Published in Nature 524, 442–445 (27 August 2015) doi:10.1038/nature14890.

This material is based upon work supported by the U.S. Department of Energy, Office of Science, Office of Basic Energy Sciences, under Contract No. DE-AC02-76SF00515.

as the muon collider[6], the laser wakefield accelerator[7] and the plasma wakefield accelerator[8] (PWFA), are under development. Of these, the PWFA has showed tens of billion electronvolt energy gain in less than one meter[9], and recently shown high-efficiency acceleration of a narrow energy spread electron bunch containing a significant charge, at a high energy gain per unit length[2] (or gradient). However, for a future PWFA-based particle collider, it is imperative to demonstrate that the antimatter counterpart of the electron (e^-), the positron (e^+), can also be accelerated in a PWFA at high gradient and with high-energy efficiency.

The longitudinal component of the electric field E_z associated with a wake produced by the passage of either an intense ultra-relativistic e^- or e^+ bunch through a plasma can, in principle, be used to accelerate positrons. In both cases, a dense ($n_b>n_p$), tightly focused ($k_p\sigma_r$ <1), short ($k_p\sigma_z$<1), ultra-relativistic (γ>>1) drive bunch (e^- or e^+) can be used to excite a nonlinear (non sinusoidal) wake in a plasma. Here n_b, n_p, k_p, σ_r, σ_z and γ are the bunch density, plasma density, wavenumber of the plasma wave, r.m.s. focused transverse spot size, r.m.s. longitudinal size and the Lorentz factor of the bunch, respectively. However, the nonlinear wakes produced by the two types of drivers are qualitatively different[1]. With an e^- driver, a region devoid of plasma electrons, called an ion cavity, is formed as these electrons are blown out by the transverse electric field of the bunch[10, 11]. Within this ion cavity, the transverse force is defocusing for positrons and so prevents positron acceleration. To get around this problem, the use of a hollow plasma channel to produce wakes without a focusing force[12-14], or the use of Laguerre-Gaussian laser pulses to drive donut shaped wakes with a strong focusing force for positrons[15], have been suggested.

In contrast to the e^--driven wake, when an otherwise similar e^+ bunch is used, plasma electrons that are radially located within a few plasma skin depths (k_p^{-1}) from the bunch are attracted inward (rather than being expelled) by the transverse electric field of the bunch[16-18]. As the plasma electrons are flowing in, positrons experience a negative or decelerating E_z, losing energy as they do work on the plasma electrons. Once most plasma electrons have crossed the propagation axis, E_z abruptly switches sign from negative to positive and becomes accelerating for positrons. If there are no positrons to sample the accelerating field, the wake is said to be unloaded as no energy is extracted from it. This is shown in Fig. 1a, taken from a simulation using the three-dimensional particle-in-cell code QuickPIC[19, 20]. In this case, plasma electrons flow outward after they cross the axis, which leads to the formation of a cavity where the ion density exceeds the electron density. When a significant number of positrons are sampling the accelerating field, a large number of electrons crossing the axis remain close to the axis (see Fig. 1b). Consequently the longitudinal and the transverse fields are both strongly altered, *i.e.* loaded. Due to the presence of the plasma electrons on axis, the loaded transverse force guides the accelerated positrons through the length of the plasma accelerator. These positrons can extract a substantial fraction of the wake's energy and alter the shape of the E_z field, which tends to become more uniform and produces a narrow energy spread peak in the accelerated part of the positron spectrum. This process occurs in the positron-driven wake without the need for a distinct trailing bunch[21]. In other words, the front of a single e^+ bunch can excite a wake in a plasma while the rear of the same bunch loads and extracts energy from this wake (as in Fig. 1b). This regime is referred to as the self-loaded plasma wakefield.

The formation of a spectrally-distinct accelerated narrow energy spread e^+ bunch was discovered in an experiment conducted at the SLAC's Facility for Advanced Accelerator Experimental Tests[22] (FACET), using its 20.35 GeV positron beam (see Methods). A single

bunch containing ~1.4×10^{10} positrons and having an r.m.s. bunch length in the range of 30-50 μm was focused to an r.m.s. transverse spot size of less than 100 μm at the entrance of a lithium plasma. The plasma is produced by laser ionization of a 1.15-m-long lithium vapour column of uniform density, that has 15-cm-long density up and down ramps on either end[23, 24] (see Methods). The electron density of the plasma was set to 8×10^{16} cm^{-3} by controlling the pressure and the temperature of the lithium vapour. After the interaction with the plasma, an imaging spectrometer consisting of a quadrupole magnet doublet, a strong dipole magnet and a Cherenkov detector[25] was used to characterize the energy spectrum of the positron beam (see Methods). The quadrupole magnet doublet was set up to image the plasma exit to the location of the detector for a given positron energy - the energy set point E_{image}. The dispersion from the dipole magnet was set high enough such that positrons with energies in a band of ~3 GeV around E_{image} are well focused (and thus accurately resolved) at the detector. To record both the decelerated and the accelerated parts of the positron spectrum, E_{image} of the quadrupole magnet doublet was varied in increments of 2.5 GeV from 10.35 GeV to 27.85 GeV.

Figures 2a and 2b show the accelerated part of the final energy spectrum of the e^+ bunch after its passage through the plasma, where E_{image} is set to 22.85 GeV and 25.35 GeV, respectively. The accelerated positrons in Figs. 2a and 2b have peaks at 24.75 ± 0.27 GeV and 26.11 ± 0.35 GeV. These two examples show that the accelerated positrons have a narrow energy peak, albeit on top of a broader "shoulder". The r.m.s. energy spread of the peaks shown in Figs. 2a and 2b are obtained by fitting an asymmetric Gaussian function to the peaks, and measured to be 1.8% and 2.2% r.m.s., respectively. The positron charge contained in the peak (under the red dashed curve) is 207 ± 14 pC for the shot of Fig. 2a and 126 ± 8 pC for the shot of Fig. 2b. We have found experimentally that the energy gain of this peak can vary shot to shot from 3 GeV to 10 GeV. The contrast between the peak and the shoulder was also varying shot to shot, and in some cases, the accelerated part of the spectrum would be flat or decreasing (see Extended Data Fig. 1). The narrowest peaks were observed when the maximum energy gain was ~5 GeV. For an acceleration length of 1.3 m, this energy gain corresponds to an average loaded gradient of ~ 3.8 GeV/m. Simulations discussed in Supplementary Information show that the peak energy and the peak-to-shoulder ratio are sensitive to σ_z, the details of the longitudinal shape of the bunch (*i.e.* the rise time versus the fall time), σ_r, and the normalized transverse emittance of the bunch (see Extended Data Fig. 2). In the experiment, several of these parameters fluctuated from one shot to the next, and it was not possible to determine which parameter affected the experimental outcome most sensitively. Nevertheless, these results demonstrate the self-formation of a narrow energy spread positron bunch with multi-GeV energy gain in a metre-scale plasma accelerator.

Figure 2c shows the decelerated part of the positron spectrum, with E_{image} set to 12.85 GeV. The spectral charge density is continuous and decreases monotonically from 20.35 GeV to less than 10 GeV. The amount of energy that is transferred to the wake is computed as the total amount of energy lost by the decelerated positrons. For the shot of Fig. 2c, a decelerated charge of 511 ± 34 pC has transferred 2.40 J of energy to the plasma wake. The energy extracted from the wake by the accelerated charge in the narrow peaks of Figs. 2a and 2b was calculated to be 0.86 J and 0.69 J, respectively. The energy extraction efficiency is obtained by taking the ratio of the energy gained by the accelerated charge contained in the peak to the energy transferred to the wake by the decelerated charge. Because the spectral charge density is only accurately measured for energies near E_{image}, the amount of energy lost by the decelerated charge cannot be determined for the shots shown in Figs. 2a and 2b. The energy extraction efficiency and its error are thus estimated using the average amount of energy loss and its shot-to-shot variation, which

are obtained using data acquired with E_{image} ranging from 10.35 to 20.35 GeV (see Methods). The resultant average amount of energy loss is found to be 2.54 J, with variations of ± 0.3 J from shot to shot. The fraction of energy extracted from the wake by the charge in the peaks of Figs. 2a and 2b are thus estimated to be 34% ± 5% and 27% ± 4%, respectively.

To interpret these experimental results, three-dimensional particle-in-cell simulations for beam and plasma parameters similar to those used in the experiment are performed with the code QuickPIC[19, 20]. In particular, the bunch has asymmetric normalized emittances in the two transverse dimensions of 200 (in x) and 50 mm.mrad (in y) respectively. Results are presented in Fig. 3. During the first 10 cm of propagation in the flat density region of the plasma, feedback of the forces exerted by the plasma on the e^+ bunch and vice versa causes the e^+ bunch and the plasma wake to rapidly evolve, until they reach a quasi-steady state. In this quasi-steady state, the longitudinal and transverse fields vary slowly in time (see Supplementary Movie 1). Figure 3a shows that after 135 cm of propagation through the plasma the initially Gaussian e^+ bunch evolves to form an arrowhead-shaped structure. Interestingly, a small number of positrons located in the region $-140 < \xi$ (μm) < -90 are focused by the plasma electrons close to the bunch axis, as seen in the on-axis positron bunch density profile of Fig. 3a. We note that in simulations with a higher initial charge and symmetric emittances, these positrons form a spatially and spectrally distinct bunch. Figure 3b shows the energy spectrum of the positrons at this point in the plasma. It shows that the initial 20.35 GeV positron bunch has both lost and gained energy. The energy loss monotonically extends down to 7 GeV but the energy gain feature shows a clear high-energy peak centred around 25 GeV, on top of a broader energy shoulder. The inset in Fig. 3b shows that most positrons with energies exceeding 24 GeV reside close to the beam axis in the region $-100 < \xi$ (μm) < -70. The transverse force (see Fig. 3c and Extended Data Fig. 3) confines positrons close to the axis in a pseudo potential well, as shown in the inset of Fig. 3c.

This large positron charge experiencing an accelerating electric field can extract a significant fraction of the energy stored in the wake. In doing so, this portion of the e^+ bunch alters substantially the shape of the wake. The simulation shows that this self-loading of the wake can result in a nearly uniform longitudinal electric field along the length of the accelerated charge. These positrons thus gain approximately the same energy, which leads to the formation of a narrow energy spread accelerated peak in the final positron spectrum (see Fig. 3b). The colour plot of the E_z field and its on-axis lineout in Fig. 3d clearly show that the peak decelerating field is larger than the peak accelerating field. Further, the volume with the highest decelerating field is small compared to the extent of the bunch. This leads to a final positron energy spectrum that has a long energy loss tail (see Fig. 3b), in good agreement with the experimental results shown in Fig. 2.

In conclusion, we have discovered a mechanism that accelerates positrons with multi-GV/m fields in a plasma. Using a nonlinear plasma wake driven by a single positron bunch, a substantial number of positrons is shown to be accelerated and guided over a metre-scale plasma. The accelerating electric fields exceed by two orders of magnitude those available with radio-frequency technology. The large number of accelerated positrons loads the wake and extracts a significant fraction of its energy. This self-loading flattens the longitudinal electric field of the wake resulting in a narrow energy spread spectrum. These results show that the PWFA concept may be a solution for an energy booster upgrade to a linear collider[26].

1. Joshi, C. & Katsouleas, T. Plasma accelerators at the energy frontier and on tabletops. *Phys. Today* **56**, 47–53 (2003).

2. Litos, M. *et al.* High-efficiency acceleration of an electron beam in a plasma wakefield accelerator. *Nature* **515**, 92–95 (2014).

3. The Particle Physics Project Prioritization Panel (P5), subpanel of the High Energy Physics Advisory Panel (HEPAP), "Building for Discovery, Strategic Plan for U.S. Particle Physics in the Global Context" (2014; http://www.usparticlephysics.org/p5/).

4. Barish, B. & Yamada, S., Eds. "The International Linear Collider Technical Design Report". ILC-REPORT-2013-040 (2013).

5. Aicheler, M. *et al.*, Eds. "A Multi-TeV linear collider based on CLIC technology: CLIC Conceptual Design Report". CERN-2012-007 (2012).

6. Alexahin, Y. *et al.* Muon Collider Higgs Factory for Snowmass 2013. In *Proceedings of the Community Summer Study 2013: Snowmass on the Mississippi* http://arxiv.org/abs/1308.2143 (2013).

7. Schroeder, C. B., Esarey, E., Geddes, C. G. R., Benedetti, C. & Leemans, W. P. Physics considerations for laser-plasma linear colliders. *Phys. Rev. ST Accel. Beams* **13**, 101301 (2010).

8. Adli, E. *et al.* A beam driven plasma-wakefield linear collider: from Higgs factory to multi-TeV. In *Proceedings of the Community Summer Study 2013: Snowmass on the Mississippi* http://arxiv.org/abs/1308.1145 (2013).

9. Blumenfeld, I. *et al.* Energy doubling of 42 GeV electrons in a metre-scale plasma wakefield accelerator. *Nature* **445**, 741-744 (2007).

10. Rosenzweig, J. B., Breizman, B., Katsouleas, T. & Su, J. J. Acceleration and focusing of electrons in two-dimensional nonlinear plasma wake fields. *Phys. Rev. A* **44**, R6189–R6192 (1991).

11. Lu, W., Huang, C., Zhou, M., Mori, W. B. & Katsouleas, T. Nonlinear theory for relativistic plasma wakefields in the blowout regime. *Phys. Rev. Lett.* **96**, 165002 (2006).

12. Lee, S., Katsouleas, T., Hemker, R. G., Dodd, E. S. & Mori, W. B. Plasma-wakefield acceleration of a positron beam. *Phys. Rev. E* **64**, 045501(R) (2001).

13. Kimura, W. D., Milchberg, H. M., Muggli, P., Li, X. & Mori, W. B. Hollow plasma channel for positron plasma wakefield acceleration. *Phys. Rev. ST Accel. Beams* **14**, 041301 (2011).

14. Yi, L. Q. *et al.* Positron acceleration in a hollow plasma channel up to TeV regime. *Sci. Rep.* **4**, 4171 (2014).

15. Vieira, J. & Mendonça, J. T. Nonlinear laser driven donut wakefields for positron and electron acceleration. *Phys. Rev. Lett.* **112**, 215001 (2014).

16. Hogan, M. J. *et al.* Ultrarelativistic-positron-beam transport through meter-scale plasmas. *Phys. Rev. Lett.* **90**, 205002 (2003).

17. Blue, B. E. *et al.* Plasma-wakefield acceleration of an intense positron beam. *Phys. Rev. Lett.* **90**, 214801 (2003).

18. Muggli, P. *et al.* Halo formation and emittance growth of positron beams in plasmas. *Phys. Rev. Lett.* **101**, 055001 (2008).

19. Huang, C. *et al.* QuickPIC: a highly efficient fully parallelized PIC code for plasma-based acceleration. *J. Phys. Conf. Ser.* **46**, 190–199 (2006).

20. An, W., Decyk, V. K., Mori, W. B. & Antonsen, T. M., Jr. An improved iteration loop for the three dimensional quasi-static particle-in-cell algorithm: QuickPIC. *J. Comput. Phys.* **250**, 165–177 (2013).

21. Tzoufras, M. *et al.* Beam loading in the nonlinear regime of plasma-based acceleration. *Phys. Rev. Lett.* **101**, 145002 (2008).

22. Hogan, M. J. *et al.* Plasma wakefield acceleration experiments at FACET. *New J. Phys.* **12**, 055030 (2010).

23. Muggli, P. *et al.* Photo-ionized lithium source for plasma accelerator applications. *IEEE Trans. Plasma Sci.* **27**, 791–799 (1999).

24. Green, S. Z. *et al.* Laser ionized preformed plasma at FACET. *Plasma Phys. Contr. Fusion* **56**, 084011 (2014).

25. Adli, E., Gessner, S. J., Corde, S., Hogan, M. J. & Bjerke, H. H. Cherenkov light-based beam profiling for ultrarelativistic electron beams. *Nucl. Instrum. Methods Phys. Res. A* **783**, 35 (2015).

26. Lee, S. *et al.* Energy doubler for a linear collider. *Phys. Rev. ST Accel. Beams* **5**, 011001 (2002).

Acknowledgements The FACET E200 plasma wakefield acceleration experiment was built and has been operated with funding from the United States Department of Energy. Work at SLAC was supported by DOE contract DE-AC02-76SF00515 and also through the Research Council of Norway. Work at UCLA was supported by DOE contracts DE-FG02-92-ER40727 and DE-SC0010064. Simulations were performed on the UCLA Hoffman2 and Dawson2 computers and on Blue Waters through NSF OCI-1036224. Simulation work at UCLA was supported by DOE contracts DE-SC0008491 and DE-SC0008316, and NSF contracts ACI-1339893 and PHY-0960344. The work of W.L. was partially supported by NSFC 11175102, the Thousand Young Talents Program and the Tsinghua University Initiative Scientific Research Program. We are grateful to P. Muggli for many fruitful discussions regarding plasma wakefield acceleration.

Author Contributions All authors contributed extensively to the work presented in this paper.

Author Information Reprints and permissions information is available at www.nature.com/reprints. The authors declare no competing financial interests. Readers are welcome to comment on the online version of the paper. Correspondence and requests for materials should be addressed to S.C. (corde@slac.stanford.edu).

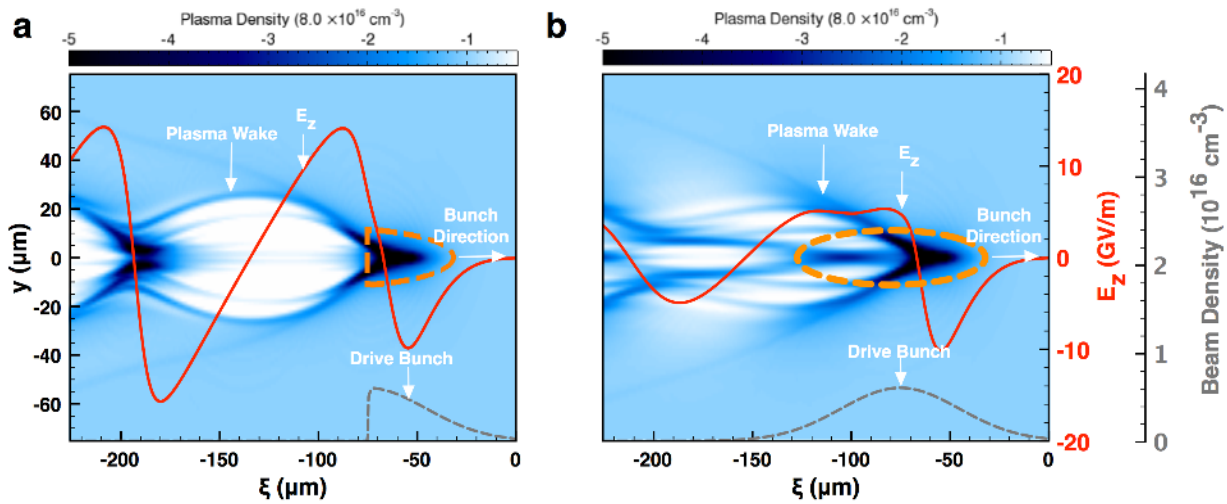

Figure 1 | Simulated plasma wakes driven by short and intense positron bunches. The electron plasma density in the (y-ξ) plane is shown after a propagation distance of 135 cm into the plasma, where y is the dimension transverse to the direction of motion of the bunch, and $\xi = z\text{-}ct$ is the dimension parallel to the motion. For each panel the one-third-maximum contour of the initial positron bunch density is represented by the orange dashed line, the on-axis density profile of the initial positron bunch is shown in grey dashed line, and the on-axis longitudinal electric field E_z is in red solid line. The beam and plasma parameters (described later in Fig. 3 caption) are the same as those in the experiment. **a**, The unloaded plasma wake, for which no positrons are being accelerated by the wake as the bunch has been terminated just as E_z reverses sign. **b**, The self-loaded plasma wake, where the trailing particles of a single bunch extract energy from the wake excited by the particles in the front.

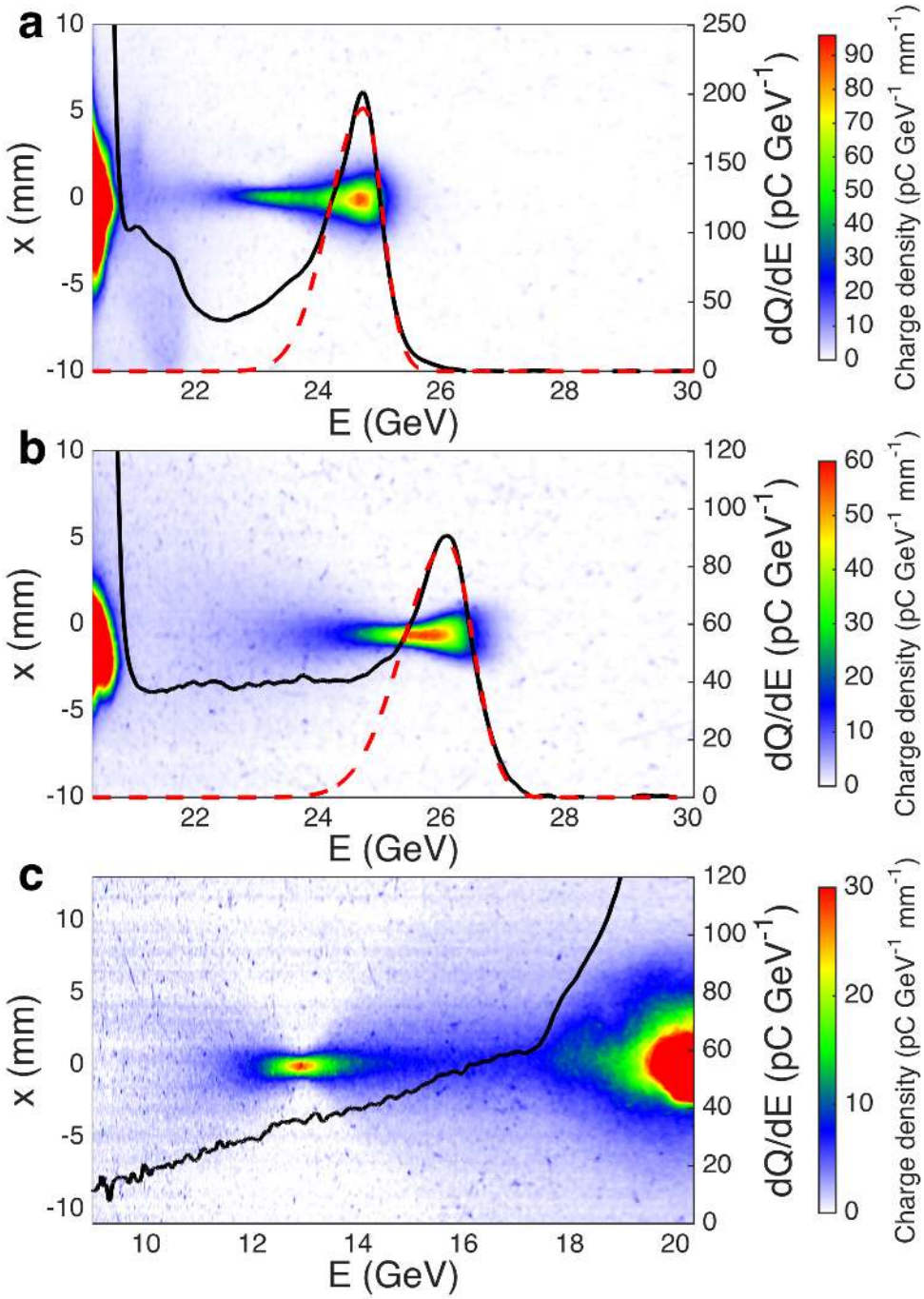

Figure 2 | Experimental positron energy spectra. **a** and **b**, Two examples of the accelerated portion of the spectrum of the positrons after the interaction with the plasma with E_{image} at 22.85 GeV (in **a**) and 25.35 GeV (in **b**). **c**, An example of the decelerated portion of the positron spectrum with E_{image} at 12.85 GeV. For all frames, the density of charge per unit energy and length of the dispersed positron beam profile is shown in colour, and the spectral charge density is represented in black solid line (right scale). Asymmetric Gaussian fits to the peaks in **a** and **b** are shown as red dashed lines. Particles that do not participate to the interaction are visible at the initial beam energy, 20.35 GeV.

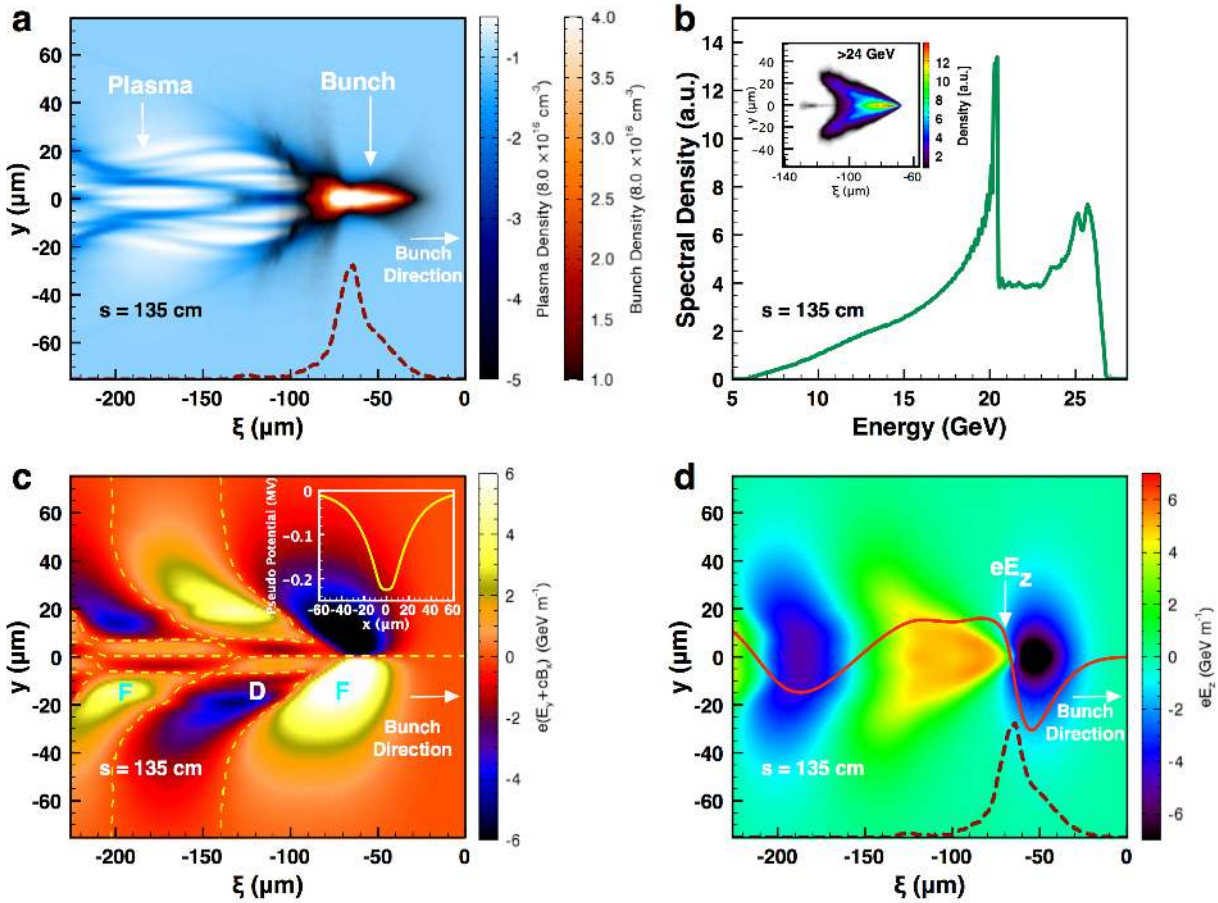

Figure 3 | Particle-in-cell simulation. **a**, Electron plasma density and positron beam density in the (y-ξ) plane. **b**, Final spectrum of the positron bunch after its interaction with the plasma. The inset shows the projected density in the (y-ξ) plane of the positrons with energies greater than 24 GeV. **c**, Transverse force $F_y \approx e(E_y+cB_x)$ experienced by the positrons. The dashed lines represent the $F_y = 0$ contour. F and D indicate respectively the focusing and defocusing regions of the wake. The inset shows a lineout of the pseudo potential ψ (given implicitly by $\mathbf{F}_\perp = -\nabla_\perp e\psi$) taken at ξ = -75 μm. **d**, Longitudinal electric field E_z. In **a** and **d**, the on-axis density profile of the positron bunch is represented in red dashed line. In this simulation, the bunch contains 1.4×10^{10} positrons and has transverse and longitudinal spot sizes of σ_r = 70 μm, σ_z = 30 μm. The bunch energy is 20.35 GeV and the plasma density is 8×10^{16} cm^{-3}.

METHODS

Positron beam. The experiment reported in this letter used the 20.35 GeV, ~2.2 nC positron bunches delivered by the FACET facility to the experimental area situated in Sector 20 (see Extended Data Fig. 4). The positrons at FACET originate from the electromagnetic shower produced when a 20.35 GeV electron beam is sent into a six-radiation-length tungsten alloy target[27]. An electron beam is therefore first accelerated in the FACET 2-km-long linear accelerator (linac), before being sent to the positron target in Sector 19. A large number of electron-positron pairs are created during the electromagnetic cascade in the target. Positrons exiting the target are captured and transported by the Positron Return Line to the start of the linac, where they are accelerated and injected into the South Damping Ring of Sector 2. After cooling the positron beam in the damping ring, the beam is accelerated in the linac and undergoes three stages of compression[12], (i) in the ring-to-linac section, (ii) in Sector 10 and (iii) in Sector 20. At the exit of the Sector 20 bunch compressor, the beam has a fully compressed bunch length in the range of 30-50 micrometers (r.m.s.), corresponding to a duration of 100-170 fs (r.m.s.). Five quadrupole magnets (the final focus system) focus the beam to a spot size of less than 100 micrometers (r.m.s.) in both transverse dimensions at the entrance of the plasma. The final focus is configured so as to have beta functions (propagation distance from the waist at which the beam size is increased by $2^{1/2}$) of 50 cm in x and 500 cm in y at focus.

Plasma source. A column of lithium vapour is confined in a heat-pipe oven by a helium buffer gas at both ends[23]. The lithium atomic density is uniform over a length of 1.15 m, and has 15-cm-long ramps on either end, giving a full width at half-maximum (FWHM) length of 1.3 m. The lithium atomic density in the plateau region is set to 8×10^{16} cm^{-3} by controlling the pressure and the temperature in the heat-pipe oven. The lithium vapour is ionized prior to the passage of the positron bunch by a Ti:sapphire laser pulse[24]. The laser has an energy of about 20 mJ, a FWHM pulse duration of 200 fs and is focused by a 0.75° axicon lens, which produces a zero-order Bessel intensity profile over the full length of the column of lithium vapour. The laser focus line is aligned to the positron bunch axis over the entire length of the oven.

Energy spectrum and efficiency. The energy of the positrons is characterized using a Cherenkov imaging spectrometer[25]. A dipole magnet, whose equivalent length and magnetic field are 97.8 cm and 0.8 T, respectively, deflects the positrons vertically. Positrons with an energy of 20.35 GeV experience a 11.46 mrad deflection. At the location of the detector, the vertical position of a positron provides a measurement of its energy. A quadrupole magnet doublet is used to image the plane where the beam exits the plasma to the location of the detector. The imaging conditions only hold for a given positron energy E_{image}. The energy resolution depends on the finite vertical beam size at the detector and on the detector resolution itself, and is of the order of 50 MeV for energies near E_{image}. The detector consists of a camera imaging the Cherenkov light produced by positrons as they pass through a 5-cm-long air gap, limited by two silicon wafers positioned at an angle of 45° to the beam. To measure the decelerated part of the positron spectrum, the dipole magnetic field is set to 0.4 T. By doing so, the detector field of view allows us to measure positrons with energies above 9 GeV.

For the accelerated portion of the energy spectrum presented in Figs. 2a and 2b, asymmetric Gaussian functions are fitted to the spectral charge density for energies above 24 and 25.25 GeV, respectively. The fits are then used to calculate the number of accelerated positrons and the amount of energy gained by the peak. For the decelerated portion of the energy spectrum presented in Fig. 2c, the decelerated charge and the amount of energy transferred to the wake are calculated using all positrons having lost more than 1 GeV. Further, the contribution of positrons

with final energies below 9 GeV (*i.e.* not detected) to the decelerated charge and the energy loss is determined using a linear extrapolation of the measured spectrum. This extrapolation accounts for about 10% of the total amount of energy loss.

To estimate the energy extraction efficiency, we divide the energy gained by the particles in the peak of Figs. 2a or 2b by the average amount of energy transferred to the wake by the decelerated particles (particles that have lost more than 1 GeV, including the extrapolation of the spectrum for energies below 9 GeV). The average energy loss is obtained using a piecewise reconstruction of the average decelerated spectrum, shown in Extended Data Fig. 5. In this reconstruction, each piece of the spectrum corresponds to the average of the ~35 spectra recorded for the given values of E_{image}, from 10.35 GeV to 20.35 GeV. The average energy loss obtained from this piecewise reconstruction is 2.54 J. It agrees within 5% with the average energy loss obtained by using only the data recorded at E_{image} = 10.35 GeV. The main error in this estimation of the energy extraction efficiency is related to the shot-to-shot fluctuation of the energy loss, which equals 0.3 J (r.m.s.) and leads to an uncertainty of ± 5% and ± 4% in the energy extraction efficiency of Figs. 2a and 2b, respectively.

Particle-in-cell simulations.

Computer simulations were carried out with the three-dimensional particle-in-cell (PIC) codes QuickPIC[19, 20], OSIRIS[28] and Hybrid OSIRIS[29]. The outcomes of all three codes, in particular the plasma wake and the beam evolution as the positron beam propagated through the plasma, were compared against one another to ensure that all three gave the same results. The results of the quasi-static QuickPIC code are presented in Figs. 1 and 3. The input bunch contains ~1.4×10^{10} positrons and has Gaussian profiles in both transverse and longitudinal dimensions, with σ_r = 70 μm and σ_z = 30 μm, and a normalized emittance of 200 and 50 mm.mrad in the two transverse dimensions. The beam has an energy of 20.35 GeV and zero initial energy spread. The plasma has a trapezoidal density profile with a uniform density of 8×10^{16} cm^{-3} over a 1.2-m-long region and 15-cm-long linear density up- and down-ramps on either side, corresponding to a FWHM length of 1.35 m. The simulation box tracks the beam-plasma interaction in the coordinates x, y and $\xi = z\text{-}ct$, that is, the box moves at light speed although it sees the plasma and the positron bunch in the laboratory frame. The box has a size of 600 μm × 600 μm × 320 μm in the two transverse dimensions and the longitudinal dimension, respectively. The number of cells in the simulation box is 512 × 512 × 512 (~ 134 million in total). A 790-frame movie of the simulation is available as Supplementary Movie 1, and shows the evolution of the longitudinal and transverse fields of the wake as the positron beam propagates through the plasma.

27. Erikson, R., Ed. "SLAC Linear Collider Design Handbook". SLAC-R-714 (1984; http://www.slac.stanford.edu/pubs/slacreports/slac-r-714.html).

28. Fonseca, R. A. *et al.* OSIRIS: A Three-Dimensional, Fully Relativistic Particle in Cell Code for Modeling Plasma Based Accelerators. *Lect. Notes Comput. Sci.* **2331**, 342 (2002).

29. Davidson, A. *et al.* Implementation of a hybrid particle code with a PIC description in r–z and a gridless description in φ into OSIRIS, *J. Comput. Phys.* **281**, 1063-1077 (2015).

SUPPLEMENTARY INFORMATION

The positron bunch parameters such as the r.m.s. transverse and longitidunal spot sizes and the normalized transverse emittance can vary in the experiment. To check the sensitivity of the results to the positron bunch parameters, additional QuickPIC simulations were carried out. The following parameters were scanned over ranges that occur in the experiment: the bunch length σ_z, the longitudinal shape of the bunch (rise time versus fall time), the transverse beam size σ_r, and the normalized transverse emittance. Parameters were varied one at a time, while keeping all the other parameters constant. Other simulation parameters are as described in Methods. The results of this simulation scan are presented in Extended Data Fig. 2, which shows the final positron spectrum for every parameter sets. Although the gross features of the wake (*e.g.* the reversing of the E_z field within the rise time of the bunch) remain the same, the peak value of the on-axis accelerating field, the on-axis plasma electron density, and the loading of the longitudinal and transverse fields do vary significantly over the range of parameters scanned in the simulations.

The effects of the scanned parameters on the beam-plasma interaction and the final positron spectrum can be summarized as follows.

a) Variation of σ_z and σ_r: In the experiment, the r.m.s. bunch sizes in the transverse and the longitudinal directions can vary by a factor of two. In the simulations, increasing σ_z or decreasing σ_r reduces the maximum energy gain and modifies the peak-to-shoulder ratio and the energy spread. An example of each is shown in Extended Data Fig. 2a.

b) Longitudinal pulse shape: The maximum energy of the positrons is quite sensitive to the details of the longitudinal profile of the bunch. For instance if the bunch has an asymmetric profile with a sharper rise and a gentler fall such that the sum of the r.m.s rise and fall times is held constant (as well as the FWHM length of the bunch), the maximum energy gain increases significantly while the peak-to-shoulder ratio is substantially reduced. For instance, as shown in Extended Data Fig. 2b (green curve), an asymmetric Gaussian bunch with a 20 μm rising edge and a 40 μm falling edge gives a peak energy gain increased by 2 GeV. The faster rise of the current profile of the bunch excites a wake of larger amplitude, which increases the energy gain.

c) Normalized transverse emittance: The final positron spectrum is quite sensitive to the input normalized transverse emittance of the bunch, as shown in the Extended Data Fig. 2c. Note that the variation of the normalized emittance is performed at constant σ_r, and therefore corresponds to a change in the width of the transverse momentum distribution of the beam. When the emittance is increased from 100×25 μm^2 to 200×50 μm^2, the decelerating field does not change as can be seen from the nearly identical decelerated portion of the energy spectrum of the positrons, but the acceleration is substantially affected. Further increasing the emittance reduces the peak decelerating field. In all cases, the beam loading is reduced as the emittance is increased, which leads to a higher energy gain, a smaller peak-to-shoulder ratio and a larger peak energy spread. The spectrum is flat and has the highest energy gain for the highest emittance.

In summary, the energy gain and the energy spread of the charge contained in the narrow spectral peak, as well as the peak-to-shoulder ratio, depend strongly on the transverse and longitudinal properties of the positron bunch. In the experiment, all these beam parameters can vary simultaneously, and one can therefore expect a wide range of outcomes, as observed in the experiment and shown in Fig. 2 and Extended Data Fig. 1.

In the Extended Data Fig. 4, we present the QuickPIC results of the case shown in Fig. 3 but in the (x-ξ) plane. The arrowhead shaped evolution of the bunch is more pronounced in this plane because the bunch emittance is larger in the x dimension.

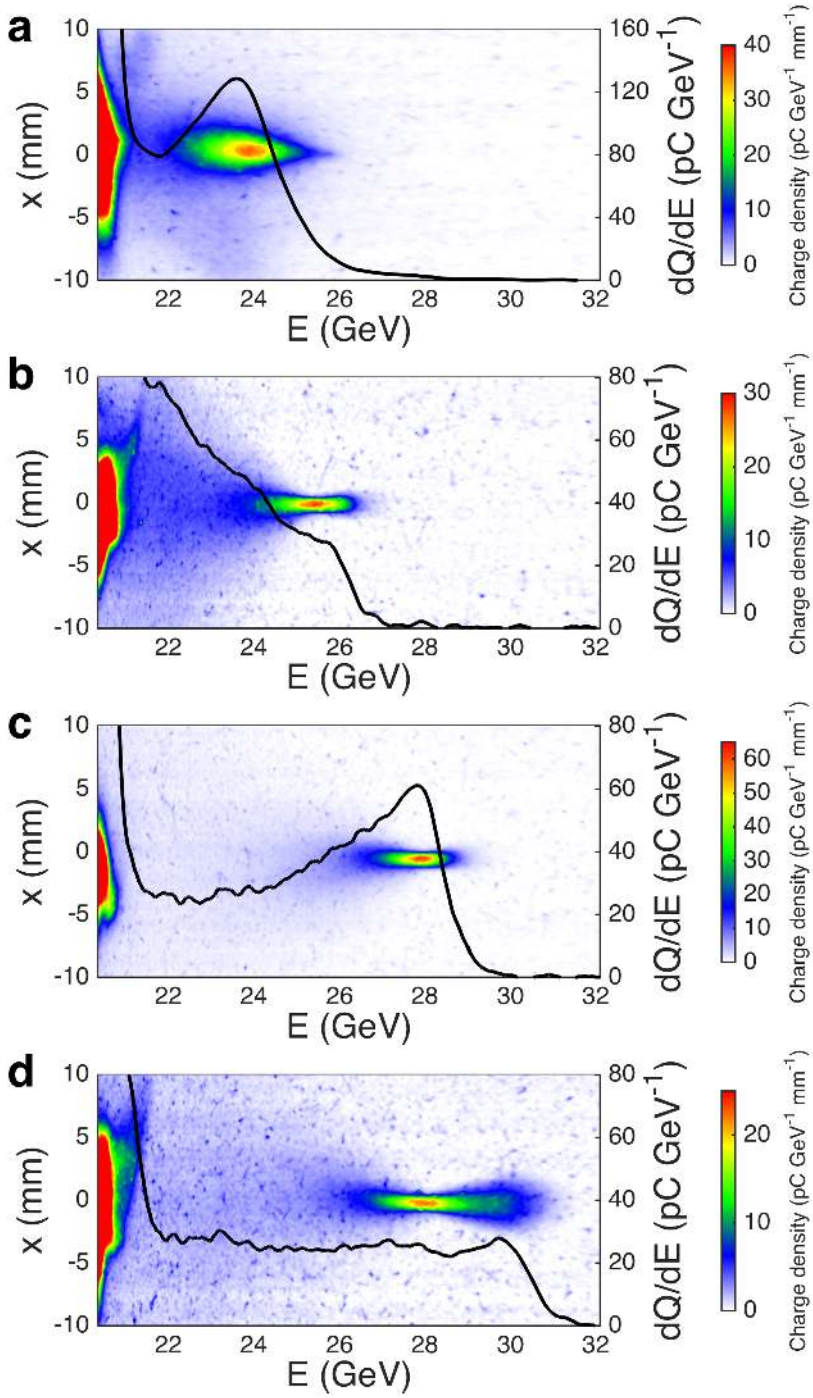

Extended Data Figure 1 | Other experimental outcomes. a-d, Various examples of the accelerated portion of the spectrum of the positrons after the interaction with the plasma, with E_{image} at 25.35 GeV (in **a** and **b**) and 27.85 GeV (in **c** and **d**). The charge density of the dispersed positron beam profile is shown in color, and the spectral charge density is represented in black solid line (right scale). The spectrum is peaked with a relatively large energy spread in **a** and **c**, is continuously decreasing in **b** and is flat in **d** for the highest maximum energy gain of ~10 GeV. Particles that do not participate to the interaction are visible at the initial beam energy, 20.35 GeV.

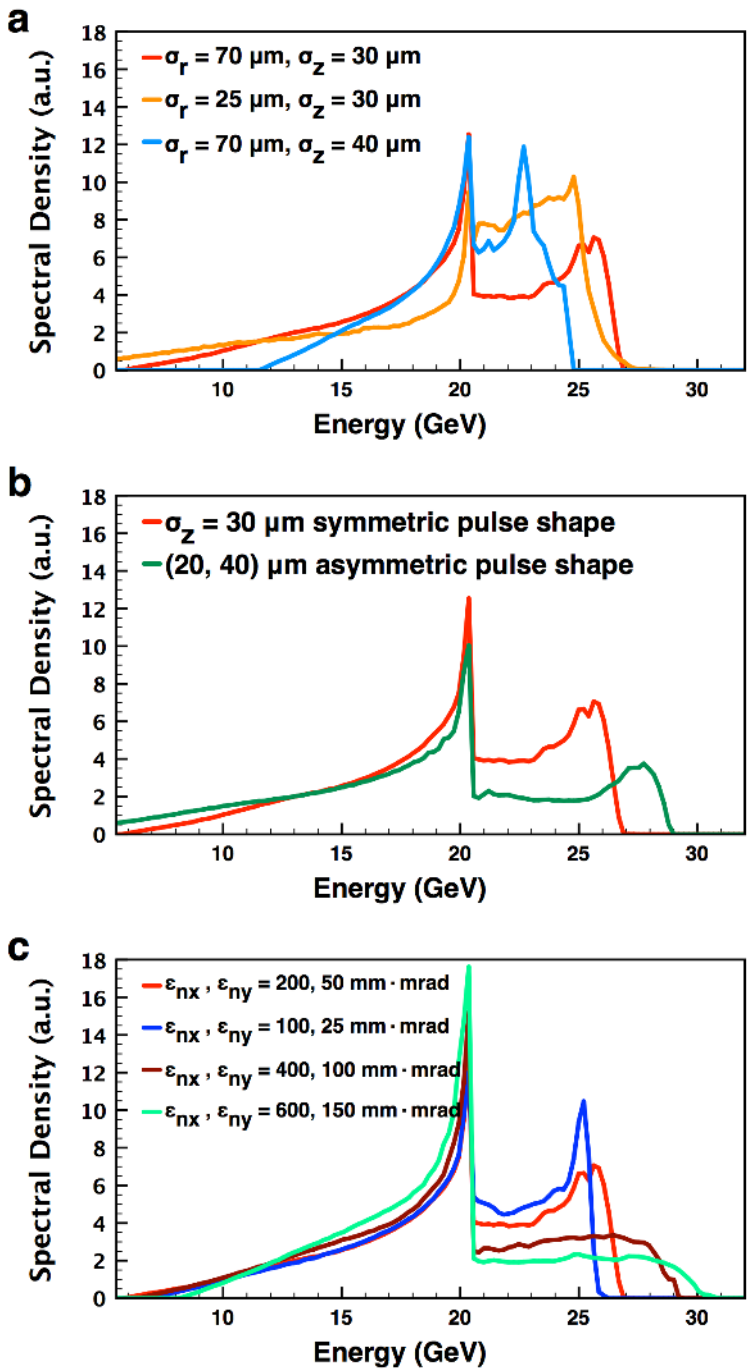

Extended Data Figure 2 | Sensitivity to bunch parameters in computer simulations. a, Final positron spectrum from QuickPIC simulations as σ_z and σ_r are varied. **b**, Final positron spectrum as the bunch longitudinal asymmetry is varied. The red (green) curve corresponds respectively to a longitudinally symmetric (asymmetric) bunch. **c**, Final positron spectrum as the normalized transverse emittance is varied, holding σ_r constant.

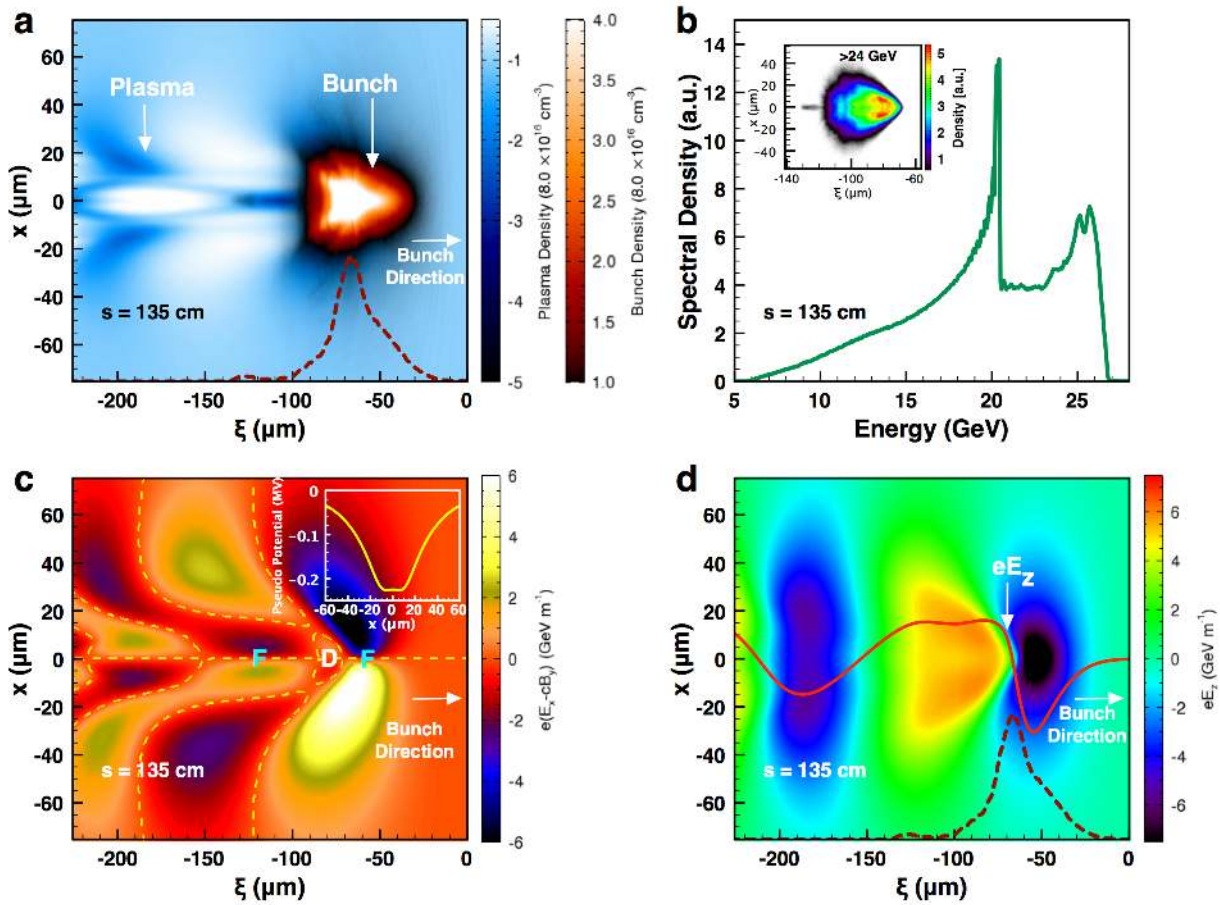

Extended Data Figure 3 | Particle-in-cell simulation results in the (x-ξ) plane. a, Electron plasma density and positron beam density in the (x-ξ) plane. **b**, Final spectrum of the positron bunch after its interaction with the plasma. The inset shows the projected density in the (x-ξ) plane of the positrons with energies greater than 24 GeV. **c**, Transverse force $F_x \approx e(E_x\text{-}cB_y)$ experienced by the positrons. The dashed lines represent the $F_x = 0$ contour. F and D indicate respectively the focusing and defocusing regions of the wake. The inset shows a lineout of the pseudo potential ψ (given implicitly by $\mathbf{F}_\perp = -\nabla_\perp e\psi$) taken at ξ = -75 μm. **d**, Longitudinal electric field E_z. In **a** and **d**, the on-axis density profile of the positron bunch is represented in red dashed line. In comparison to the (y-ξ) plane shown in Fig. 3, here the transverse force is slightly defocusing close to the axis in the region -85 < ξ (μm) < -70. The emittance being larger in x, the beam evolves toward a larger spot size along this dimension. As a result, the on-axis plasma electrons that provide the focusing force take a marginally longer time to reach the x=0 plane, which leads to a small region where the force is locally slightly defocusing. Nevertheless, the positrons remain confined and guided by the pseudo potential well, as seen in the inset of **c**.

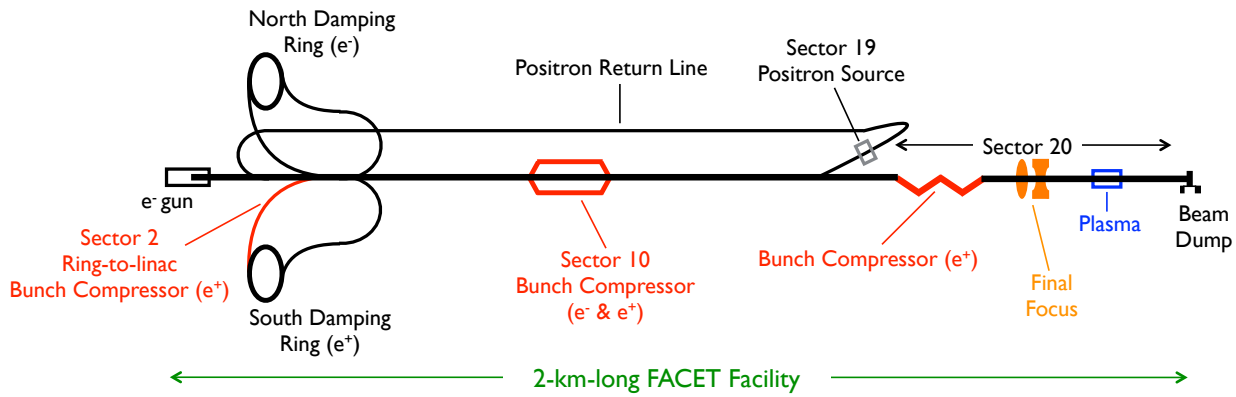

Extended Data Figure 4 | Schematic of the FACET facility. Positrons are created in the positron source of Sector 19, transported to the start of the linac by the Positron Return Line, and cooled in the South Damping ring. They are then accelerated in the linac and compressed in the ring-to-linac section, in Sector 10 and in Sector 20, and are focused by the final focus system to the entrance of the plasma in Sector 20.

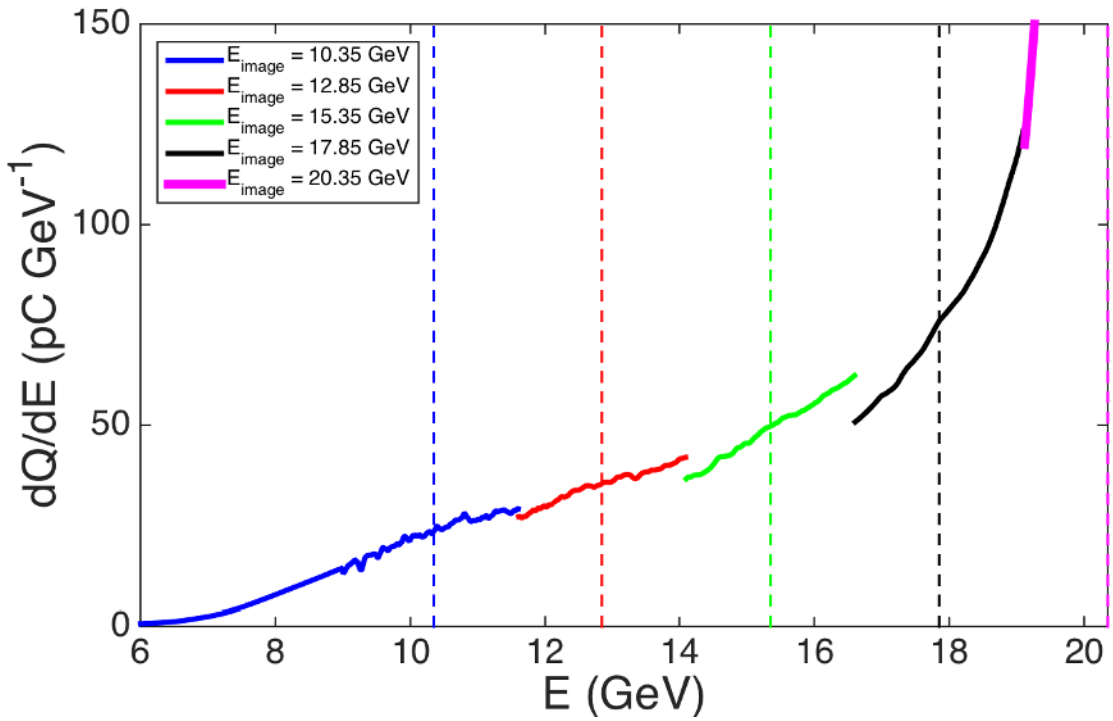

Extended Data Figure 5 | Piecewise reconstruction of the decelerated part of the average positron spectrum. Each piece of the reconstructed spectrum is the average of ~35 spectra measured at a given quadrupole energy set point E_{image}. E_{image} = 10.35 GeV is represented in blue solid line, E_{image} = 12.85 GeV in red solid line, E_{image} = 15.35 GeV in green solid line, E_{image} = 17.85 GeV in black solid line and E_{image} = 20.35 GeV in magenta solid line. Except for the two extreme energy set points, each piece of the reconstruction covers a 2.5 GeV energy range centered around its energy set point. Single shot spectra are linearly extrapolated for energies below 9 GeV, and this extrapolation is accounted for in the blue curve. The energy set points are represented in dashed line.